JOURNAL OF OPTOELECTRONICS AND ADVANCED MATERIALS Vol. 10, No. 4, April 2008, p. 929 - 932

High density MgB_2 superconductor: structure and morphology through microtomography and SEM investigations

GH. –V. ALDICA*, P. NITA[b], I. TISEANU[a], T. CRACIUNESCU[a], P. BADICA
National Institute of Materials Physics, Bucharest-Magurele, Romania
[a]*National Institute for Lasers, Plasma and Radiation Physics, Bucharest-Magurele, Romania*
[b]*METAV SA, Bucharest, Romania*

Recently, MgB_2 was discovered to be a superconductor with a surprisingly high critical temperature of about 39 K and with significant potential for applications. This material is usually prepared from a mixture of Mg and B in sealed tubes with excess Mg. As-prepared samples usually are very porous and mechanically weak. High density superconducting samples of MgB_2 undoped and doped with SiC and B_4C were produced by Field Assisted Sintering Technique (FAST) (T_c = 38.5 K). Samples are relatively large of 1.9 cm in diameter, apparently uniform, and can be easily extracted from the die. Processing times are short for easily attainable and relatively low temperatures. The effects of FAST consolidation on crystalline morphology revealed by microtomography and Scanning Electron Microscopy (SEM) and bulk density were investigated. Most samples have bulk density above 90% of the theoretical one. Despite such high bulk density, microtomography in combination with SEM revealed that in the samples there are some regions of low and high density. High density regions are not the consequence of FAST processing and they were observed in the raw material.

(Received February 25, 2008; accepted April 2, 2008)

Keywords: SEM, X-ray μ-tomography, MgB_2 superconductor, Microstructure

1. Introduction

Magnesium diboride represents an attractive alternative to low temperature superconductors which still dominate the low temperature large scale applications of superconductivity [1-3]. In addition to a satisfactory critical temperature T_c and the extremely transparent grain boundaries, MgB_2 also displays a unique potential to increase the upper critical H_{c2} and irreversibility H_{irr} fields by appropriate doping.

One promising method to obtain a dense MgB_2 superconductor is the Field Assisted Sintering Technique (FAST) that was successfully used to consolidate different kinds of difficult-to-sinter powders [4-7]. In this technique, the sample is submitted to a pulsed electric field during the compression process. Although the physics involved is not completely understood, this method provides an excellent way to obtain high density MgB_2 [8-10], while preventing the increase of the grain size. Both, high density and reduced size, are very important features for maximization of the properties in MgB2. In this regard detailed study of the microstructure of MgB_2 samples is of interest.

The influence of raw materials, doping and FAST sintering conditions on microstructure of the samples were investigated through microtomography in combination with electron microscopy (SEM) techniques. This study showed the samples are different from this point of view.

2. Experimental

Polycrystalline samples of MgB_2 (MB), C-doped MgB_2 (MBBC), and SiC-doped MgB_2 (MBSC) were prepared from commercially available powders of MgB_2 (2.3 μm, Alpha Aesar), SiC (45 nm, Merck), and B_4C (0.8 μm, HC Starck Grade HS). In the case of doped samples, the molecular ratio between MgB_2 and dopant was 95/5. Samples were sintered using a "Dr Sinter" (Sumitomo Coal Mining Co, Japan) machine. The preparation details were published elsewhere [11].

The density was calculated from measured mass and specimen size using a 0.1 mg Mettler Toledo balance (AB204-S type) and a 0.001 mm digital Mitutoyo micrometer.

Micro-tomographic experiments were performed on the high resolution X-ray micro-tomography facility constructed at the Association EURATOM-MEdC (Romania) with European Community support [12]. The main component is an open type microfocus X-ray source (maximum high voltage of 160 kVp at 20W maximum power). X-rays are detected by means of a large area, high-resolution image intensifier or an amorphous silicon flat panel sensor. The detection system is placed on a precise motorized stage additionally provided with vertical and transversal manually adjustable table. The investigated sample is placed on a motorized micrometric manipulator to assure maximum degree of freedom in sample positioning. The micro-radiography analysis is guaranteed for feature recognition down to 1 micron. Due to the ability to work with maximum magnifications over 1000, it has been demonstrated that for the individual miniaturized samples the micro-tomography analysis is valid for feature recognition down to few microns.

The 3D tomographic reconstructions are obtained by OCVB, a proprietary highly optimized computer code [13], based on a modified Feldkamp algorithm [14]. As the X-ray detector is mounted on a micrometric manipulator, a special

technique based on random movement by a number of camera pixels, was used as an efficient method to reduce the ring artifacts in the reconstructed cross-sections. Adequate software [15] can be used to navigate inside the 3D reconstruction.

The MgB_2's fracture surfaces have been studied using a Hitachi S-2600N SEM.

3. Results

The FAST pellets have bulk densities (Table 1) above 90 % of the theoretical value (2.6 g/cm^3). For 0.95 MgB_2+0.05B_4C a smaller density is observed probably due to the limited chemical reaction between two components, and to a lower sintering temperature.

Tabel 1. The FAST temperature, density and T_d data.

Sample	T(°C)	Density (g/cm^3)	T_d (°C)
MB	960	2.39	920
MBSC	1000	2.37	955
MBBC	1000	2.08	960

The tomographic inspection was performed using the following operation parameters: U = 50 kV, I = 40 mA, voxel size = 5 μm). Representative results on the pristine MgB_2 sample are presented in Figs. 1 – 3. Fig. 1 illustrates the identification of high density regions inside the investigated sample. By filtration and thresholding techniques the distribution of these high density regions inside the volume of the sample is revealed (Fig. 2). The identification of macroscopic low density regions is illustrated in Fig. 3.

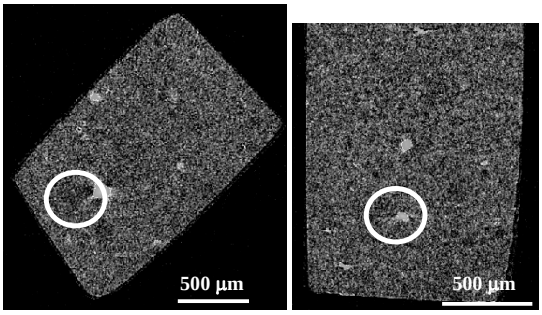

Fig. 1. Transversal and sagital cross-sections revealing high density regions; high density region size inside marker: ~ 160 μm.

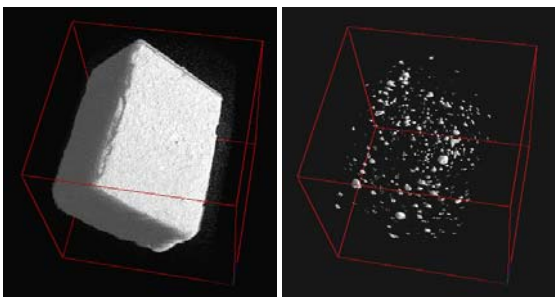

Fig. 2. 3-D reconstruction (left) and the distribution of the high density regions inside the volume of the sample.

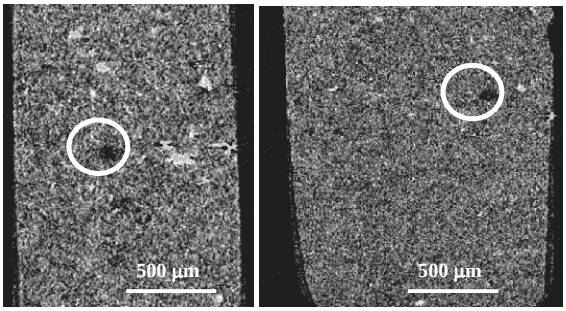

Fig. 3. Sagital and longitudinal cross-sections revealing low density region; low density region size inside marker: ~ 130 μm.

To identify what represent these dense regions, the high resolution X-ray digital radiography analysis was performed on the raw powder sample. The result is presented in Fig. 4. In order to have a dimensional reference, a wolfram wire, 5 μm diameter, was placed on the sample. The radiography reveals high density regions, of above 2-3 μm diameter-size, spreaded in the sample. Same intensity of the W-wire and of the high density regions suggests that in the commercial as-received MgB_2 raw powder this element is present, most probably in the form of WC. We suppose that impurification occured during powders milling in the process of commercial MgB_2 raw powder preparation.

Similar images (not presented) were observed in SiC- and B_4C- doped MgB_2 samples. There are no significant differences from the microtomography measurements viewpoint. For further in depth investigation of microstructure that requires a higher resolution we used SEM.

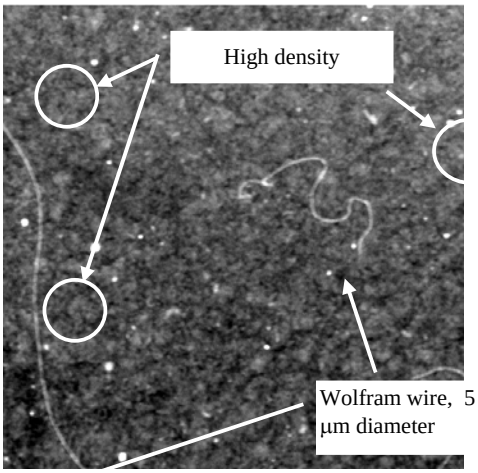

Fig. 4. Digital radiography.

Before the study by SEM, the samples have been fractured to reveal their grains structure and morphology. Selected secondary electron images are shown in Figs. 5-7. One can observe dense polycrystalline pristine material with pores and grains of different form and size (Fig. 5). The pores of micrometer order are located at the grain boundaries. Size of the grains is of 0.5 – 2.5 μm.

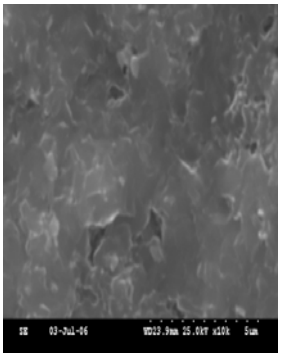

Fig. 5. Polycrystalline MgB_2 sample (×10.000).

The B_4C-doped MgB_2 samples (Figs. 6 and 7) are composed of many aggregates of grains in ellipsoidal form with average axis length of 40 and 150 μm (Fig. 6). The morphology of aggregates can be observed in detail in Fig. 7.

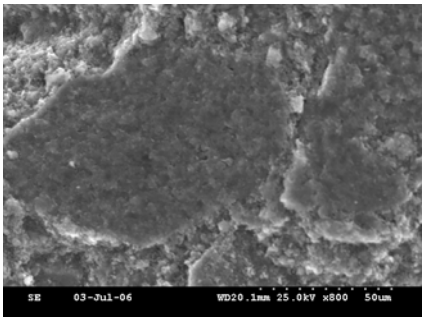

Fig. 6. The aggregates of grains in B_4C-doped MgB_2 sample (×800).

Fig. 7 shows also a skeleton-like arrangement with a high degree of porosity having small pores (0.5 - 1 μm), located at the grain boundaries.

The fractured surface of SiC doped MgB_2 sample is slightly different (Fig. 8): the grains have a large size distribution. Actually, some grains are not quite clearly defined and larger melt-like areas surrounded by tiny particles ranging from few nanometers to several micrometers are present. Connectivity between individual small particles is rather poor.

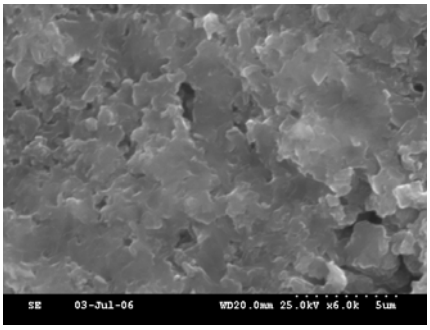

Fig. 7. The morphology of the aggregates of grains in B_4C-doped MgB_2 sample (×6.000).

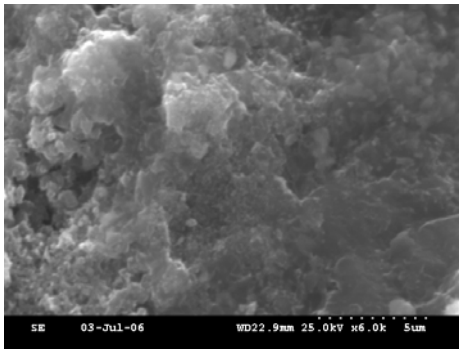

Fig. 8. SiC-doped MgB_2 sample fracture surface (×6.000).

4. Discussion

The onset temperature (T_d) of the densification process is lower for MgB_2 sample, and higher for the doped superconductor samples (see Table 1). This T_d value seems influenced by the rheological properties at high temperatures of the doping material in the guest matrix (MgB_2). The difference in the T_d values is reflected in the density and microstructure of the samples. It is interesting that, although for the doped samples showing a higher T_d we applied a higher FAST processing temperature (1000°C for samples MBSC and MBBC instead of 960°C for sample MB) these samples could not attain the highest density of the pristine sample as well as the best microstructural uniformity and connectivity observed for the same sample. To reveal the reason for such behaviour more research is required. However, our results indicate that for our three samples, FAST processes are developing in a different manner. One should consider carbon diffusion into MgB_2 lattice and specific features of FAST such as creation of hot spots, enhancement of (electro)diffusion, development of states close to plasma, all of them significantly reflected in the way the grain boundaries are formed and, hence, on the microstructure and properties of the superconductor.

5. Conclusions

We have shown that combination between 3D μtomography, a technique suitable to observe relatively large volumes and local surface analysis through SEM is very useful to observed microstructure of MgB_2 samples. In this work we investigated doped (SiC and B_4C) and undoped samples of MgB_2-bulk prepared by FAST.

It is shown that samples have different characteristics of density, local density and microstructure pending on raw materials, dopants and processing conditions.

All FAST MgB_2-samples of relatively large size (1.9 cm) had bulk density above 90% of the theoretical one, except those doped with B_4C. This result suggest that FAST is a promising method for further developments on MgB_2 superconductor.

The best FAST sample from the density and microstructure viewpoints was the un-doped MgB_2 sample.

Acknowledgments

One of the authors (G. Aldica) is grateful for Research Scholar support of this work from University of California at Davis, U.S.A. This work is supported by NSF and is performed under CEEX 27/2005 program.

References

[1] J. Nagamatsu, N. Norimasa, T. Muranaka, Y. Zenitani, J. Akimitsu, Nature **410**, 63 (2001).
[2] D. C. Larbalestier, et al 2001 Nature **410**, 186 (2001).
[3] H. Fang, P. Gijavanekar, Y. X. P Zhou, P. T. Putman, K. Salama, 2005 IEEE Trans. Appl. Supercond. **15**, 3200 (2005).
[4] J. R. Groza, ASM Handbook Vol. **7**: Powder Metal Technologies and Applications, eds. P. W. Lee, W.B. Eisen, R. M. German (ASM International Handbook Committee, Ohio), pp. 583-589 (1998).
[5] M. Omori, Mater. Sci. Eng. A **287**, 183 (2000).
[6] M. Tokita, 1999 Mater. Sci Forum **308-311,** 83 (1999).
[7] E. M. Carrillo, C. Unvar, J. C. Gibeling, G. H. Paulino, Z. A. Munir, Scripta Mater. **45**, 405 (2001).
[8] S. Y. Lee, S. Y. Yoo, Y. W. Kim, N. M. Hwang, D. Y. Kim, J. Am. Ceram. Soc. **86**, 1800 (2003).
[9] K. J. Song, C. Park, S. W. Kim, R. K. Ko, H. S. Ha, H. S. Kim, S. S. Oh, Y. K. Kwon, S. H. Moon, S. –I. Yoo, Physica C **426-431**, 588 (2005).
[10] A. M. Locci, R. Orru, G. Cao, S. Sanna, F. Congiu, G. Concas, AIChE Journal **52**(7), 2618 (2006).
[11] G. Aldica, P. Badica, J. R. Groza, J. Optoelec. & Adv. Mater. **9**(6), 1742 (2007).
[12] I. Tiseanu, EFDA Fusion Newslett. **6**(4), 7 (2003).
[13] I. Tiseanu, T. Craciunescu, N. B. Mandache, Fus. Eng. Des. **75–79**, 1055 (2005).
[14] L. A. Feldkamp, L. C. Davis, J. W. Kress, J. Opt. Soc. Am. **A-1**, 612 (1984).
[15] VGStudioMax, Volume Graphics GmbH, Heidelberg, Germany, www.volumegraphics.com.
[16] R. A. Ribeiro S. L. Bud'ko C. Petrovic, P. C. Canfield, Physica C **384** 227 (2003).

*Corresponding author: aldica@infim.ro